doi: 10.5937/SimTerm24084E

Improving Flow Homogeneity in the Chambers of the Electrostatic Precipitator of a 350 MW Unit and Reduction of Particulate Matter Emissions by Modifying the Turning and Damping Elements

Milić D. Erić [a], Zoran Marković [b], Predrag Stefanović [c] Aleksandar Milićević [d]
Ivan Lazović [e]

[a] *Vinca Institute of Nuclear Sciences – National Institute of the Republic of Serbia - University of Belgrade, RS, milic@vinca.rs*
[b] *Vinca Institute of Nuclear Sciences – National Institute of the Republic of Serbia - University of Belgrade, RS, zoda_mark@vinca.rs*
[c] *Vinca Institute of Nuclear Sciences – National Institute of the Republic of Serbia - University of Belgrade, RS, pstefan@vinca.rs*
[d] *Vinca Institute of Nuclear Sciences – National Institute of the Republic of Serbia - University of Belgrade, RS, amilicevic@vinca.rs*
[e] *Vinca Institute of Nuclear Sciences – National Institute of the Republic of Serbia - University of Belgrade, RS, ivan.lazovic@vinca.rs*

Abstract: In order to protect nature, legal regulations on environmental protection are becoming ever stricter. The increasing development of exhaust gas cleaning technologies has led to quick solutions and ever shorter deadlines for the reconstruction and modernization of electrostatic precipitators. This has led to problems in the operation of electrostatic precipitators over a long period of time after reconstruction and to a lower efficiency of the plants. This paper presents the optimization of flue gas flow in the electrostatic precipitator chambers of the 350 MW unit after reconstruction. During the overhaul of the thermal power plant, the distribution of air velocities in the cross-section of the chambers was investigated and the results were used to validate the numerical model. A new conceptual solution was proposed based on the results of several numerical simulations of the flue gas velocity distribution for different configurations of turning and damping elements. The partuculate matter concentration was reduced from over 70 mg/Nm^3 to a value below 35 mg/Nm^3 after the modification and modernization.

Keywords: ESP chamber, Distribution of velocities, Cross-section, Homogeneity of the flow field.

1. Introduction

Electrostatic precipitation is one of the most practical methods for separating coal dust and ash particles from the flue gas stream in thermal power plant boilers. The separation of coal dust and ash particles significantly reduces the negative impact of these waste materials on the ecosystem and human health. Worldwide standards, which are also accepted in this country, require emission limit values (ELV) of less than 50mg/m^3, in some European countries even less than 25mg/m^3. As the limit values are expected to fall further in the near future, this is the right time to develop acceptable and promising technologies and to develop new energy-efficient technologies to reduce emissions of flue gases and other pollutants (sulphur oxides, nitrogen, ...) [1, 2]

To meet these requirements, it is necessary to simultaneously increase the active surface area of the electrodes, improve the distribution of the flue gases to achieve a uniform distribution profile of the flue gases and reduce the erosive effect of the dust particles, which together increase the volume and weight of the flue gases, or even use a high-frequency high-voltage (HF HV) supply [3] instead of a transformer and diode rectifier (T/R) set. The performance of an electrostatic precipitator is usually determined by the voltage-current (V-I) characteristic, which affects the precipitation efficiency of the electrostatic precipitator and is highly dependent on the calorific value of the coal, the ash content of the coal and the electrical resistance of the ash, which in turn depends on the alkali and sulphur content of the ash [4] by affecting the current when a reverse corona occurs.

As part of the capital overhaul of Unit 2 of the KOSTOLAC-B thermal power plant in 2012, the electrostatic precipitator plant was reconstructed and modernized with the primary aim of keeping the total particulate matter (PM) concentration at the outlet of the plant below the emission limit value (ELV) of 50 mg/Nm3 (at standard conditions: dry flue gas at standard conditions and an oxygen content of 6%), which was prescribed by national (regulation in force at the time of reconstruction) and European regulations (EU Directive 2001/80/EC) [1, 5].

After completion of the guarantee tests, where the condition that the measured concentration is below the emission limit value is fulfilled, there was an increase in the particle concentration at the outlet of the electrostatic precipitator. The annual reports on periodic testing of emissions from unit B2 for 2015 and 2016 show that the output concentration of particulate matter was well above the permitted value of the ELV. In December 2015, a particulate matter concentration of 118 to 122 mg/Nm^3 was measured [6]. Two tests were carried out in 2016: A particulate matter concentration of 110÷115 mg/Nm^3 was measured in May and 132÷140 mg/Nm^3 in December [7, 8].

TPP Kostolac has made great efforts to improve the operation of the electrostatic precipitator plant and significantly reduce concentrations. In November 2017, concentrations of 75÷79 mg/Nm^3 were measured, in 2018 it was 74÷76 mg/Nm^3 [9, 10]. In 2019, the concentrations measured were 69÷72 mg/Nm3 and in 2020 66÷70 mg/Nm^3 [11-14].

Since the concentration of particulate matter could not be reduced below the emission limit value, the Joint Stock Company Joint Stock Company Elektroprivreda Srbije, Kostolac Thermal Power Plants Branch, conducted a public tender to carry out an analysis of the condition of the electrostatic precipitator, experimental tests of the air flow and a CFD analysis of the flue gas flow in the chambers, on the basis of which the homogeneity of the flow field can be determined and improved in order to increase the efficiency of the electrostatic precipitator.

2. Basic information and analysis of the condition of electrostatic precipitator

The reconstructed electrostatic precipitator consists of two units, each with a chamber divided into four mechanical dedusting zones, the first two of which (zones 1 and 2) are divided into two electrical fields fed by high frequency devices (20 kHz), while fields 3 and 4 are fed by transformer rectifier units of the traditional 50 Hz type. In total, there are 6 independent electric fields in the left chamber and 6 in the right chamber. The basic technical data of the electrostatic precipitator and the design parameters of the unit, boiler, fuel and flue gas at the inlet of the electrostatic precipitator are given below.

Table 1. Project Parameters of Boiler Operation, Quality of Coal and Flue Gas at the Inlet to the ESP TEKO B2

Parameter	Unit	Value
Nominal power of the unit	MW_e	348,5
Nominal steam production of the boiler	t/h	1000
Pressure of the superheated steam	bar	186
Temperature of the superheated steam	°C	540
Lower calorific value of the coal	kJ/kg	6590
Moisture content of the coal	%	44,10
Ash content of the coal	%	23,9
Sulfur content of the coal	%	1,17
Carbon content of the coal	%	20,0
Hydrogen content of the coal	%	1,87
Oxygen and nitrogen content of the coal	%	8,96
Dry flue gas flow for an existing ESP: *Average coal quality* *Poorer coal quality*	m^3/h, suvi	 1 442 392 1 506 800
Flue gas temperature: normal/max/min	°C	180/200/150
Particulate matter concentration at the inlet to the ESP (0 ºC, 1013 mbar, dry gas with O_2=6%): normal/max.	g/Nm^3	67,1/75,6
Particulate matter concentration at the exit of the reconstructed ESP (0 ºC, 1013 mbar, dry gas with O_2=6%)	mg/Nm^3	≤50
Static pressure drop of the flue gas at the inlet/outlet of the ESP	mbar	≤2,5

The characteristic parameters of the electrostatic precipitator reconstructed in 2012 are: two chambers, 2*4 mechanical zones for ash separation, 12 independent electric fields (Figure 1), 24 separate hoppers for ash collection. The active height of the electric field is 15.5 m, and the active length of the electric field is 16 m (four dedusting zones of 4 m each). The distance between the electrodes for the gas passage is 400 mm in zones 1 and 2 and 500 mm in zones 3 and 4. In zones 1 and 2 there are 2*20=40 passages for the gas, in zones

3 and 4 2*16=32 passages. The total area of the collecting electrodes is 35.712 m2. The cross-sectional area for the flue gas flow is 2*248=496 m2. The maximum velocity of the flue gas in the electric field is 1.8 m, the minimum dwell time in the electric field zone is 9 s [14].

The flow of an incompressible fluid in chambers/channels with changing duct cross-sections (with diffusers and confusers) and in channels with bends and elbows was investigated both for single-phase flows (gas only) and for two-phase systems (gas with particles) and from the point of view of the uniformity of the velocity field behind the diffuser/confuser and the bends/elbows as well as from the point of view of the pressure drop in such ducts, both theoretically and experimentally.

In order to reduce the velocity of the flue gas flow from 17 m/s at the inlet to the diffuser (cross-section 3.5m*9m) to 1.5÷1.8 m/s, the designer of the new filter has created as uniform a velocity distribution as possible in the electrostatic precipitator chamber (cross-section 16.78m*16m) a short flat diffuser with a scattering angle of 2*48°=96° in the horizontal plane and scattering angles of 56° upwards and 54° downwards in the vertical plane of the diffuser.

In the front part of the diffuser there are two horizontal and five vertical turning plates and axially behind them, at a mutual longitudinal distance of 900 mm, three further walls made of perforated plates in the form of vertical plates with circular openings with a relatively large diameter of Ø85 mm. The turning plates divide the flow in the diffuser into smaller scattering angles. The turning plates divide the flow in the diffuser into smaller scattering angles.

To eliminate the vertical component of the flue gas velocities (towards the ceiling/floor of the chamber), there are seven turning plates in the upper half of the diffuser behind the second wall with a length of 155 mm (in the axial direction along the chamber axis) and an angle of -50° (in relation to the vertical), which divert part of the flue gas flow downwards. In the lower half of the diffuser, in front of the third wall, there are 7 turning plates with a length of 155 mm (in the axial direction along the chamber axis) and an angle of +50° (in relation to the vertical), which direct part of the flue gas flow upwards.

Due to their geometry and dimensions, these turning plates only partially eliminate the vertical component of the flue gas velocity (resulting in an uneven velocity profile across the height of the chamber) and significantly increase the intensity of the turbulence, which also has a negative impact on the efficiency of particle matter separation in the electrostatic precipitator. The lateral-horizontal component of the flue gas velocity at the diffuser outlet is not eliminated, resulting in an uneven velocity profile across the width of the chamber.

To equalize the distribution of velocities along the vertical and horizontal sides of the chamber, damping plates are placed in the confuser and turning vanes in the elbow at the outlet of the chamber to eliminate the uneven suction effect of the flue gas fan through the central outlet duct. According to the original documents, the designer did not provide for the installation of turning vanes in the elbow of the exhaust duct.

Between September 2018 and July 2019, the Vinca Institute conducted a study at the Kostolac B thermal power plant entitled "Analysis of the situation and possibilities for increasing the efficiency of the electrostatic precipitator in unit 2" (the first phase of research).

In this study, an analysis of the design values of the basic parameters of the electrostatic precipitator of unit B2 and a comparative analysis of the design and operating parameters of the electrostatic precipitators of thermal power plants on lignite with a capacity of 300÷350 MW in the joint-stock company Electric Power Company of Serbia and TPP Ugljevik were carried out. All electrical parameters in all electrical fields showed stable values during all tests and were in the upper range of the design values.

As part of the study, the velocity distribution in the cross-section of the electrostatic precipitator chamber the was measured. In this measuring section, seven velocities per height were measured in 14 gas passages in each chamber, resulting in a grid of 98 measuring points in total.

During the measurement of the velocity distribution in the cross-section of the electrostatic precipitator chamber, the boiler and unit B2 were not in operation. For this measurement, the flue gas and fresh air fans were switched on with the usual operating parameters for the operation of the plant, but in such a way that an average velocity of ≈1÷2 m/s was achieved in the cross-section of the ESP chamber.

The results of the measurement of the velocity distribution in the cross-section of the left and right chambers of the ESP outside the first dedusting zone performed in 2018, indicate an unsatisfactory uniformity of the velocity field. The relative standard deviation of the measured velocities is over 50 % and should be reduced to less than 25 % by this work [15].

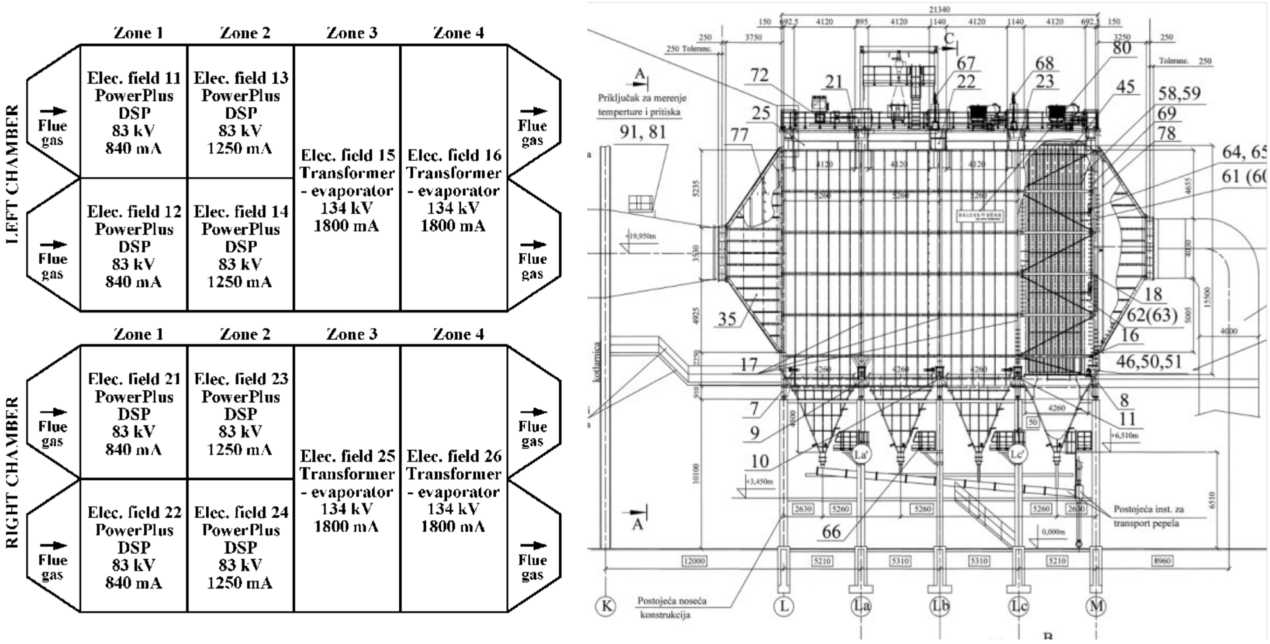

Figure 1. Arrangement of zones and electric fields in the electrostatic precipitator of unit B2

In order to achieve the required high dedusting performance and to increase the uniformity of the flue gas velocity profile in the cross-section of the electrostatic precipitator chambers, the first step was to analyse the existing condition of the inlet/outlet ducts, turning and damping elements in the electrostatic precipitator chambers (the second phase of research).

The turning elements in the chamber under the rotary air heater were reconstructed in 2005. Damage to these elements caused by the erosion of fly ash is regularly repaired as part of the annual repairs (Figure 2).

The condition of the turning and damping elements in the ESP diffuser is shown in Figure 3. In particular, the turning plates at the entrance of the diffuser and the first wall of the damping plates in the electrostatic precipitator diffuser (viewed in the direction of the flue gas flow) show considerable damage due to the erosion of the fly ash, which significantly impairs the flow pattern in the chamber, i.e. there is an uneven distribution of velocities in the cross-section of the electrostatic precipitator chambers.

Figure 2. The condition of the turning elements under the rotary air heater

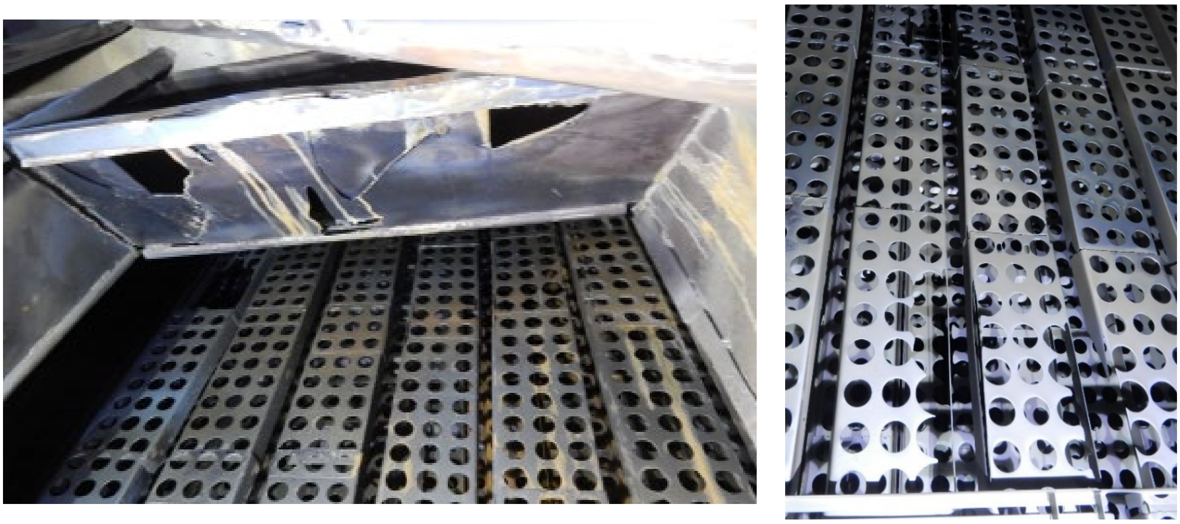

Figure 3. Damage to turning and perforated plates at the diffuser inlet

3. Results of the velocity profile measurements in the ducts upstream of the ESP chambers

The vertical measuring cross-section for measuring the velocity distribution in the cross-section of the flue gas duct in front of the electrostatic precipitator is located behind the wall of the boiler room and in front of the diffuser at the entrance to the electrostatic precipitator chamber. The 6.2 m x 4.95 m cross-section of each flue gas duct is divided into 36 equally sized areas in which the velocities are measured in the middle of each new area (the second phase of research).

Standard methods were used to measure the velocity profile in the flue gas ducts upstream of the electrostatic precipitator: The flue gas flow rate was determined according to the SRPS EN ISO 16911-1 and SRPS ISO 10780 standards, the content of O_2 and CO_2 in the flue gas according to SRPS ISO 12039, the content of CO in the flue gas according to SRPS EN 15058 and the content of H_2O in the flue gas according to SRPS EN 14790. Three tests were carried out for each flue gas duct.

Figure 4.a for Test 1 shows the corresponding 2D velocity distribution in the measurement section of the left flue gas duct upstream of the ESP. The results show that the velocity field in the measurement cross-section is shifted to the left. Figure 4.b for Test 3 shows the 2D velocity distribution in the measurement cross-section of the right flue gas duct upstream of the ESP. It can be seen that the velocity field in the measurement cross-section is shifted to the right. These shifts of the velocity fields to the outside of the flue gas ducts result from the asymmetrical flue gas outlets from the rotary air heater and hardly can be corrected by deflecting plates in the flue gas ducts at the entrance to the ESP chambers.

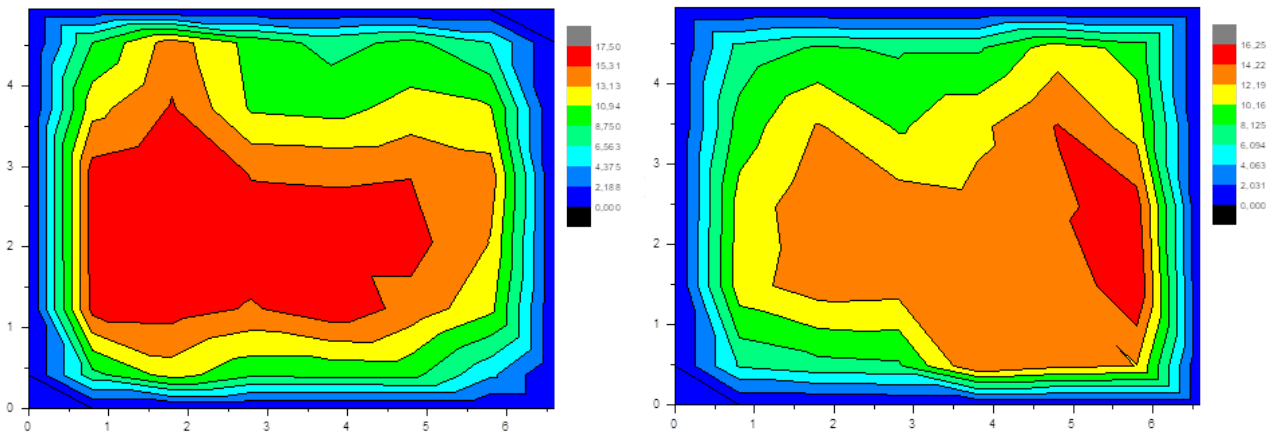

a. left duct in front of the ESP, Test 1 *b. right duct in front of the ESP, Test 3*

Figure 4. 2D distribution of velocities in the measuring section of the flue gas duct upstream of the ESP

The homogeneity of the flow field in the measured cross-section of the flue gas duct upstream of the ESP chamber was evaluated quantitatively using the following parameters: coefficient of variation CV, linear homogeneity coefficient γL1, quadratic homogeneity coefficient γL2, dimensionless coefficient of the amount of motion (Boussinesq coefficient Mk), dimensionless coefficient of kinetic energy (Coriolis coefficient Nk). According to the criterion of the coefficient of variation CV (CV≤25%), which is the most stringent, the values were between 23.5% and 27.1%, which shows that the homogeneity of the velocities in the measurement section is satisfactory in the limit range. According to other criteria, the homogeneity of the current field is satisfactory [16].

4. CFD analysis of the flow in the chamber and in the ducts upstream and downstream of the ESP chamber

The model represents the complete geometry of the structure of an ESP chamber according to the technical documentation: with an inlet duct at the exit of the boiler room, a system of 5 vertical and 2 horizontal turning plates at the entrance to the diffuser, 3 walls with perforated plates in the diffuser, a chamber with 4 dedusting zones : in the first two zones with 2*20 gas passages forming separating electrodes at a distance of 400 mm, in the last two zones with 2*16 gas passages forming separating electrodes at a distance of 500 mm and with a central vertical space for the support beams of the roof, confuser with damping vertical plates and outlet duct.

The geometry of the flow chamber (inlet duct, EF chamber and outlet duct) is completely symmetrical with respect to the central vertical longitudinal plane, so that only one half of the vertical longitudinal plane was simulated by numerical simulation in order to reduce the required computer resources (memory and time). of the side wall, Figure 5 The coordinate origin lies in the plane of the measurement section (with the measurement openings behind the boiler chamber wall) of the inlet duct, i.e. in the vertical longitudinal plane, i.e. in the vertical longitudinal symmetry plane and in the middle of the duct height, with the x (+) axis oriented in the direction of the flue gas flow along the longitudinal chamber axis, the y (+) axis along the height and the axis along the width EF, Figure 5. The flue gas flow was calculated as isothermal (180°C) with initial conditions in the inlet duct according to nominal flow values and actual parameters according to measurements in the inlet duct (Chapter 3).

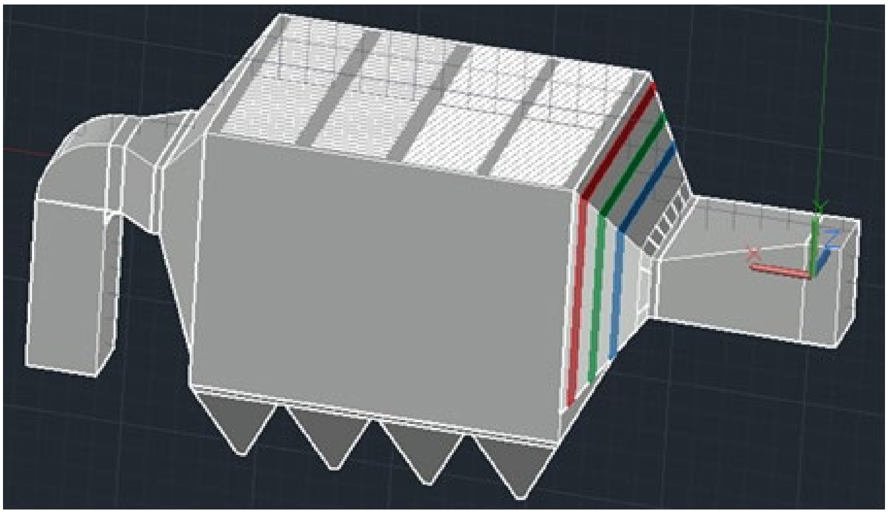

Figure 5. Model geometry for ESP

The CFD analysis of the incompressible fluid flow through the flue gas ducts upstream of the ESP, the ESP chamber and the flue gas duct downstream of the ESP of unit B2 was carried out using the ANSYS CFX 2020 R2 software package, which is based on the method of discretization of the three-dimensional flow domain with finite volume elements. The problem of single-phase isothermal steady-state turbulent 3D (three-dimensional) flow of an incompressible gas through the flow space of a closed contour is described by the time-averaged Navier-Stokes equations of Reynolds for the conservation of mass, momentum, energy, kinetic energy of turbulence and its dissipation. The discretization of the nonlinear partial transport differential equations using the first order Eulerian feedback scheme is performed for each of the variables for the steady state by establishing the equilibrium of the conventional flux, the diffusive flux and the source of the variables in the observed final volume. The field of variables computed in the nodes of the finite volume is applied using the high-resolution differential scheme of Barth and Jesperson, and the shape function of the finite element is approximated to the integration points of the finite volume element. Two additional equations for the turbulent kinetic energy and the dissipation of the turbulent kinetic energy are used to close this system of equations in the form of the standard turbulence model k-ϵ extended for the 3D case. The calculation of the value of the velocity components was performed in a "non-shifted grid" so that the control volumes are identical for all transport equations. By applying the alternative discretization method of Rhie and Chow's continuity equation and introducing the term for the pressure redistribution, the coupling of the continuity equations and the amount of motion, i.e. the pressure field and the velocity field, was performed.

The formation and calculations of the numerical models of the flow through the channels and the ESP chamber were performed on a 64-bit computer configuration Intel® Xeon® CPU E3-1231 v3 4 Cores 8 Threads 8MB Intel® Smart Cache at 3.40 GHz with 32GB DDR3 RAM under the operating system Windows Server 2019 Essentials using the ANSYS CFX 2020 R2 software within the ANSYS Workbench 2020 R2 workspace with an ANSYS Academic Associate CFD license. The geometry of the numerical model was created using FreeCad 0.18, ANSYS SpaceClaim and ANSYS DesignModeler software for 3D modeling. A numerical finite volume mesh was created using the ANSYS Workbench 2020 R2 Mesh module. The definition of the properties of the fluid (flue gas), the boundary and initial conditions in the model, the properties of the numerical calculation (advective and interpolation schemes, shape functions, turbulence model, coupling model of pressure and velocity fields, convergence criteria), the calculation of the numerical model created and the presentation of the results obtained are carried out using ANSYS CFX 2020 R2 software [17-19].

The symmetry boundary condition of the model is that the velocity component perpendicular to the plane of symmetry must be zero. The conditions in the finite volumes located up to the wall - the boundary of the domain - are described in the so-called "wall functions", both for velocities and for scalar quantities, where the walls were considered to be ideally smooth. As a convergence criterion for the iterative solution of the differential equation system, it was adopted that the normalized sum of the residuals of all finite volumes in the flow space should be smaller than 10^{-4} above a certain size.

To verify the CFD model, the results of the measurement of the velocity distribution in the cross-section of the ESP chamber upstream of the first electric field with the air flow with the flue gas fan and fresh air fan switched on were used. The optimum geometry of the turning and damping elements in the ESP chamber and in the outlet duct was determined using an iterative procedure. A CFD analysis was carried out for each of the proposed solutions (the second phase of research).

The new version of the model with the existing turning plates at the beginning of the diffuser (2 horizontal and 5 vertical) includes the following conceptual solutions:

- a new solution with three perforated walls with new smaller rectangular openings, but at the same axial positions in the diffuser as in the original solution,
- a new solution with horizontal and vertical turning plates inserted between the perforated walls,
- a new arrangement of damping vertical plates in the diffuser,
- a system of turning vanes in the elbow at the exit of the ESP chamber, which was not exist in the original solution.

Figure 6 shows the flow lines (lines along the vector of the flue gas velocity) in the entire volume from the measuring plane in the inlet duct to the measuring plane in the duct at the outlet of the ESP in the right half of the chamber of EF unit B2. The color of the currents corresponds to the intensity of the velocity vector at this point according to the attached color scale in the picture on the left. A satisfactory velocity field was obtained: very uniform in the chamber ESP with velocities running in the direction of the longitudinal axis of the chamber and minimal flow outside the zones of influence of the electric field (ceiling zone, chamber floor zone, i.e. the funnel zone and the zone in the central vertical channel where they are carriers of the chamber roof). The proposed new horizontal/vertical plates in the diffuser completely eliminate the transverse component of the flue gas velocity generated by the existing turning plates at the beginning of the diffuser and the wall jets formed on the end faces of all three perforated walls until they enter the full cross-section of the chamber.

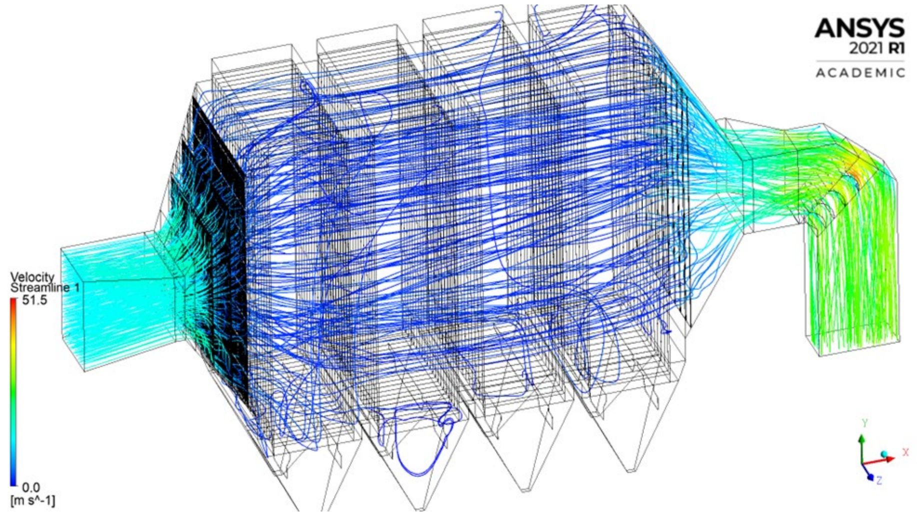

Figure 6. Intensity of the flue gas velocity (according to the corresponding color on the scale on the left) along the flow lines in the ducts upstream/downstream of the ESP and in the ESP chamber

A more detailed analysis of the flow in the chamber obtained by numerical simulation for this variant of the model was performed by showing the intensity field of the axial component of the velocities (in the x-direction along the axis of the chamber) in nine vertical and eight horizontal planes at different distances from the vertical and horizontal axial planes of the chamber. An example of the distribution of the axial component of the velocity in the vertical longitudinal plane at a distance of 3.28 m from the axis of the chamber is shown in Figure 7.

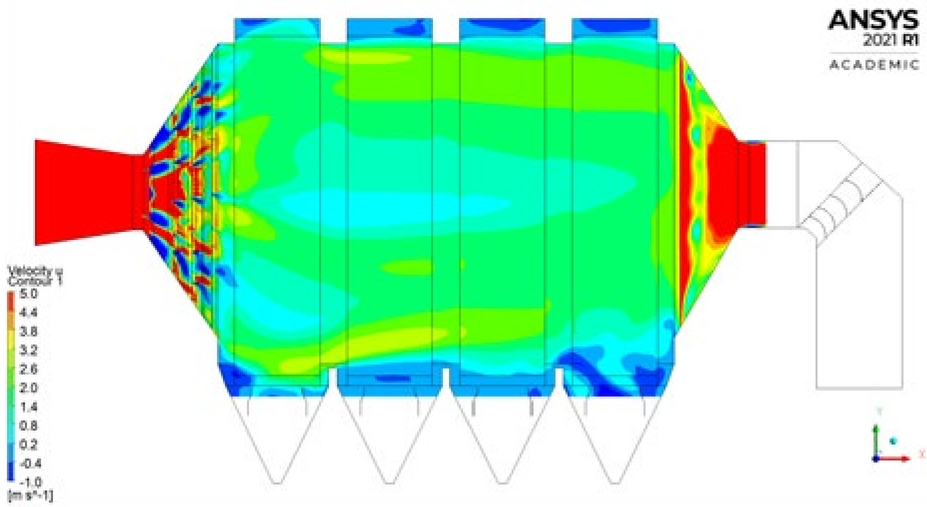

Figure 7. Distribution of the axial component of velocity in the vertical longitudinal plane at a distance of 3.28 m from the axis of the chamber

The flue gas flow at the height of the chamber is very uniform and parallel to the axis of the chamber, i.e. there is no pronounced flow towards the ceiling and from the ceiling or towards the funnels. It can be concluded that the conceptual solution of the geometry of the horizontal and vertical plates in the perforated walls 1, 2 and 3 completely eliminates the transverse component of the velocity at the outlet of the diffuser and in many ways helps to reduce the intensity of turbulence, all of which should contribute to improving the efficiency of the electrostatic precipitator.

An example of the distribution of the axial velocity component in the horizontal longitudinal plane, 2 m below the axis of the diffuser, is shown in Figure 8. The inlet duct and the diffuser are on the right-hand side, the confusor and the outlet duct on the left side of the figure. The results show that the defined geometry and arrangement of the turning/damping plates in the diffuser and confusor lead to a satisfactory uniformity of velocities across the width of the chamber at almost all height levels of the chamber.

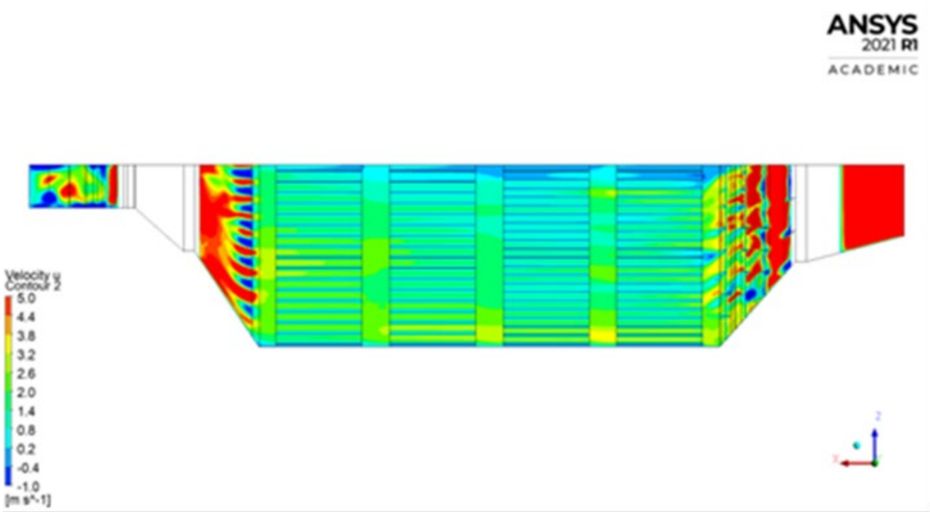

Figure 8. Distribution of the axial velocity component in the horizontal longitudinal plane, 2 m below the axis of the diffuser

The distribution of the intensity of the axial velocity in the diffuser and in the first part of the chamber is determined by the geometry of the five vertical turning plates at the beginning of the diffuser and the geometry of the perforated walls 1, 2 and 3 - and the system of vertical plates in these walls. In the second half of the chamber, the distribution of the axial velocity intensity over the cross-section of the chamber is mainly determined by the geometry/arrangement of the damping plates in the confusor. The results presented show that the defined geometry and arrangement of the turning/damping plates in the diffuser and confusor lead to a satisfactory uniformity of velocities across the width of the chamber at almost all height levels of the chamber.

The selected optimum geometry of the turning and damping elements was the basis for the creation of detailed documentation for the derived elements, according to which new elements were manufactured and installed in the electrostatic precipitator as part of the overhaul work.

The choice of the optimal solution was confirmed by the results of periodic measurements of particulate matter emissions at the outlet of the electrostatic precipitator in June and November 2021. In June, particulate matter concentrations of 31 to 38 mg/Nm3 were measured, and during the test, the electric field of the first zone in the chambers had problems with operation and could not work at 100% [20]. In November, particulate matter concentrations of 28 to 32 mg/Nm3 were measured after additional work was carried out to eliminate problems with the electrical fields in the first zone of the chambers [21].

6. Conclusions

After completion of the guarantee tests, where the condition that the measured concentration is below the emission limit value is fulfilled, there was an increase in the particle concentration at the outlet of the electrostatic precipitator. TPP Kostolac has made great efforts to improve the operation of the electrostatic precipitator plant and significantly reduce concentrations.

The increase in the efficiency of the electrostatic precipitator plant was carried out in two phases, i.e. in two large projects. In the first phase, an analysis of the design values of the basic parameters of the electrostatic precipitator of unit B2 and a comparative analysis of the design and operating parameters of the electrostatic precipitators of lignite-fired power plants were carried out. In addition, experimental investigations were carried out on the velocity distribution in the cross-section of the electrostatic precipitator chamber and in the vertical measurement cross-section in the cross-section of the flue gas duct upstream of the electrostatic precipitator. Based on these results, the homogeneity of the flow field in the measurement cross-sections was determined and these results were used to verify the CFD model.

In the second phase of the research, an analysis of the existing condition of the inlet and outlet ducts, the turning and damping elements in the electrostatic precipitator chambers was first carried out.

The optimum geometry of the turning and damping elements in the ESP chamber and in the exhaust duct was determined iteratively. The new version of the model with the existing turning plates at the beginning of the diffuser (2 horizontal and 5 vertical) includes the following conceptual solutions:

- a new solution with three perforated walls with new smaller rectangular openings, but at the same axial positions in the diffuser as in the original solution,
- a new solution with horizontal and vertical turning plates inserted between the perforated walls,
- a new arrangement of damping vertical plates in the diffuser,
- a system of turning vanes in the elbow at the exit of the ESP chamber, which was not exist in the original solution.

The CFD analysis of the incompressible fluid flow through the flue gas ducts upstream of the ESP, the ESP chamber and the flue gas duct downstream of the ESP of unit B2 was carried out using the ANSYS CFX 2020 R2 software package. A satisfactory velocity field was obtained: very uniform in the ESP chamber with velocities running in the direction of the longitudinal axis of the chamber and minimal flow outside the zones of influence of the electric field.

The proposed new horizontal/vertical plates in the diffuser completely eliminate the transverse component of the flue gas velocity generated by the existing turning plates at the beginning of the diffuser and the wall jets formed on the end faces of all three perforated walls until they enter the full cross-section of the chamber.

The choice of the optimal solution was confirmed by the results of periodic measurements of particulate matter emissions at the outlet of the electrostatic precipitator after the overhaul and installation of new elements. The particulate matter concentration measured at the outlet of the electrostatic precipitator is well below the emission limit values and is twice as high as the particulate matter concentration measured before the reconstruction.

Acknowledgements

The research was funded by the Ministry of Science, Technological Development and Innovation of the Republic of Serbia (Contract Annex: 451-03-66/2024-03/200017). The authors are very grateful for the support of this work by the Joint Stock Company Elektroprivreda Srbije.

References

[1] Directive 2001/80/EC of the European Parliament and of the Council of 23 October 2001 on the limitation of emissions of certain pollutants into the air from large combustion plants.
[2] REGULATION ON THE LIMIT VALUES FOR THE EMISSION OF POLLUTANTS INTO THE AIR FROM COMBUSTIOIN PLANTS, "Official Gazette of the RS", No. 6/2016 and 67/2021.
[3] High Frequency Power Supply for Electrostatic Precipitators in Thermal Power Plants, Slobodan Vukosavić, Electronics, Vol. 15, No. 1, June 2011, pp. 11-20.
[4] Chandra A., Enhancement of Collection Efficiencies of Electrostatic Precipitators: Indian Experiments. In: Yan K. (eds) Electrostatic Precipitation. Springer, Berlin, Heidelberg, 2009,DOI: 10.1007/978-3-540-89251-9_4
[5] REGULATION ON THE LIMIT VALUES FOR THE EMISSION OF POLLUTANTS INTO THE AIR, "Official Gazette of the RS", No. 71 of October 4, 2010.
[6] Erić, M., Marković, Z., Periodic Measurement of Pollutant Emissions in the Air of Unit B2 of the Kostolac Power Plant in Kostolac, Technical Report NIV-LTE-593, Vinča Institute, December 2015, Belgrade-Vinča.
[7] Erić, M., Marković, Z., Periodic Measurement of Pollutant Emissions in the Air of Unit B2 of the Kostolac Power Plant in Kostolac, Technical Report NIV-LTE-600, Vinča Institute, May 2016, Belgrade-Vinča.
[8] Erić, M., Marković, Z., Periodic Measurement of Pollutant Emissions in the Air of Unit B2 of the Kostolac Power Plant in Kostolac, Technical Report NIV-LTE-611, Vinča Institute, December 2016, Belgrade-Vinča.
[9] Erić, M., Marković, Z., Periodic Measurement of Pollutant Emissions in the Air of Units B1 and B2 of the Kostolac Power Plant in Kostolac, Technical Report NIV-LTE-622, Vinča Institute, November 2017, Belgrade-Vinča.
[10] Erić, M., Marković, Z., Periodic Measurement of Pollutant Emissions in the Air of Units B1 and B2 of the Kostolac Power Plant in Kostolac, Technical Report NIV-LTE-632, Vinča Institute, May 2018, Belgrade-Vinča.
[11] Erić, M., Marković, Z., Periodic Measurement of Pollutant Emissions in the Air of Units B1 and B2 of the Kostolac Power Plant in Kostolac, Technical Report NIV-LTE-649, Vinča Institute, June 2019, Belgrade-Vinča.
[12] Erić, M., Marković, Z., Periodic Measurement of Pollutant Emissions in the Air of Units B1 and B2 of the Kostolac Power Plant in Kostolac, Technical Report NIV-LTE-655, Vinča Institute, December 2019, Belgrade-Vinča.

[13] Erić, M., Marković, Z., Periodic Measurement of Pollutant Emissions in the Air of Units B1 and B2 of the Kostolac Power Plant in Kostolac, Technical Report NIV-LTE-662, Vinča Institute, July 2020, Belgrade-Vinča.
[14] Erić, M., Marković, Z., Periodic Measurement of Pollutant Emissions in the Air of Units B1 and B2 of the Kostolac Power Plant in Kostolac, Technical Report NIV-LTE-669, Vinča Institute, January 2021, Belgrade-Vinča.
[15] Stefanović, P., Erić, M., Marković, Z., Analysis of the situation and possibilities for increasing the efficiency of the electrostatic precipitator at unit 2, Version 1.0, Study, NIV-LTE-665, Vinča Institute, June 2019, Belgrade-Vinča. .
[16] Stefanović, P., Marković, Z., Erić, M., CFD model and numerical analysis of the flow in the channels upstream and downstream of the electrostatic precipitator of unit B2 TPP Kostolac, Version 1.0, Technical Report NIV-LTE-665, Vinča Institute, September 2020, Belgrade-Vinča.
[17] [19]Marković, Z., Erić, M., Jovanović, R., Lazović, I., Numerical Simulation of the Gas Flow Through the Rectangular Channel With Perforated Plate, Thermal Science, Year 2023, Volume 27, Issue 3, pp 2241 – 2253.
[18] Marković, Z., Erić, M., Stefanović, P., Jovanović, R., Lazović, I., Optimization of the Flue Gas Flow Controlling Devices of the Electrostatic Precipitator of Unit 4 In TPP "Nikola Tesla", Thermal Science, Year 2023, Volume 27, Issue 5, pp 3591 – 3606.
[19] Marković, Z., Erić, M., Stefanović, P., Lazović, I., Milićević, A., Mančić M., Jovčevski, M., Jovanović, R., Investigation of velocity distribution in channels and chambers of the electrostatic precipitator at TPP Nikola Tesla Unit A1, Thermal Science, Year 2023, Volume 27, Issue 6, pp 4877 – 4892.
[20] Erić, M., Marković, Z., Periodic-Control Measurement of Pollutant Emissions in the Air of Unit B2 of the Kostolac Power Plant in Kostolac, Technical Report NIV-LTE-677, Vinča Institute, June 2021, Belgrade-Vinča.
[21] Erić, M., Marković, Z., Periodic Measurement of Pollutant Emissions in the Air of Unit B2 of the Kostolac Power Plant in Kostolac, Technical Report NIV-LTE-682, Vinča Institute, December 2021, Belgrade-Vinča.